Resolution function for controlled-source seismic interferometry: a data-driven diagnosis

Joost van der Neut and Jan Thorbecke University of Technology*

Summary

With controlled-source seismic interferometry we can redatum sources from their actual locations at the earth's surface to downhole receiver locations without requiring a velocity model. Traditionally, interferometry is based on time-reversal arguments or a reciprocity theorem of the correlation type. Alternatively, we can interpret the retrieved Green's functions as approximate solutions of a more general inverse problem. We take the latter route to derive a resolution function for interferometry that can be estimated directly from the data if multiple downhole receivers are available. The resolution function can be used to predict virtual source radiation characteristics, the emergence of spurious events and data blurring. To demonstrate these concepts, we analyze the resolution function for a synthetic salt flank example. We show how the resolution function can help us in selecting effective tapers to the source array, which is a common practice in the application of controlled-source interferometry.

Introduction

Seismic interferometry offers an effective base for data-driven redatuming of source locations to downhole receiver locations (Wapenaar et al., 2008a; Schuster, 2009). It allows us to bypass near-surface problems, broaden illumination and improve repeatability in time-lapse surveys. Applications include salt-flank imaging (Hornby et al., 2007; Ferrandis et al., 2009), virtual crosswell imaging (Minato et al., 2007) and monitoring below complex and/or changing overburden (Bakulin and Calvert, 2006). Traditionally, interferometry has been derived from a reciprocity theorem of the correlation type or time-reversal arguments (Wapenaar et al., 2005). Variations include the virtual source method, where the direct field is time-gated prior to correlation (Bakulin and Calvert, 2006), interferometry with decomposed fields (Mehta et al., 2007; van der Neut and Wapenaar, 2009), interferometry by single-station deconvolution (Vasconcelos et al., 2008a) and various types of target-oriented interferometry (Vasconcelos et al., 2008b). Another branch of interferometry that recently emerged starts from a reciprocity theorem of the convolution type. A forward convolution-based equation is derived, which is inverted in a least-squares sense. This type of methodology has been referred to as multi-dimensional deconvolution (Wapenaar et al., 2008b), which is closely related to Betti deconvolution (Holvik and Amundsen, 2005) and least-squares redatuming (Schuster and Zhou, 2006). To apply interferometry by multi-dimensional deconvolution, some type of wavefield separation needs to be applied prior to inversion. Classically, this separation is done by acoustic or elastic decomposition (Wapenaar et al., 2008b). Another option is to time-gate the direct field (van der Neut, 2009). We start with general expressions for interferometry by cross-correlation and (multi-dimensional) deconvolution, following Wapenaar et al. (2008c). From these expressions we derive a resolution function for interferometry that can be estimated directly from the observed data. Some applications are demonstrated with a synthetic salt flank example.

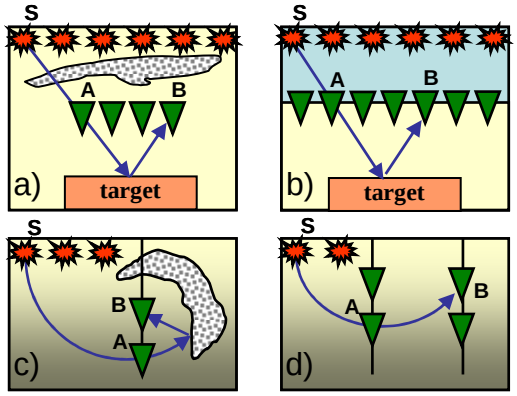

Figure 1: Four types of interferometric redatuming; a) imaging below complex overburden; b) ocean bottom cable redatuming; c) salt flank imaging; d) virtual crosswell imaging.

Data-driven redatuming by cross-correlation

In Figure 1 four types of problems are indicated, where interferometry can play an important role in redatuming wavefields. In all cases, the sources are redatumed from their actual locations **S** to virtual locations **A**, coinciding with the receivers. In interferometry, this is generally done by cross-correlation of two wavefields and integration over sources, which can be expressed in the space-frequency domain (denoted by the hat) as (Wapenaar et al., 2008c)

$$\hat{C}(\mathbf{x}_B \mid \mathbf{x}_A) = \int_{S_S} \hat{W}(\mathbf{x}_S)\,\hat{u}(\mathbf{x}_B \mid \mathbf{x}_S)\,\hat{v}^*(\mathbf{x}_A \mid \mathbf{x}_S)\,d\mathbf{x}_S\,. \qquad (1)$$

Here $\hat{C}(\mathbf{x}_B \mid \mathbf{x}_A)$ is the retrieved response between virtual source location $\mathbf{x}_A$ and receiver $\mathbf{x}_B$; superscript $*$ denotes complex conjugation. Integration takes place over the boundary S_S of source positions $\mathbf{x}_S$. $\hat{u}$ and $\hat{v}$ are full or partial wavefields, depending on the type of

interferometry that is applied. One choice is for both $\hat{u}$ and $\hat{v}$ to be full two-way wavefields (Wapenaar et al., 2005). In the virtual source method, $\hat{v}$ is the time-gated direct field and $\hat{u}$ the full or scattered field (Bakulin and Calvert, 2006). For decomposed data (Mehta et al., 2007; van der Neut and Wapenaar, 2009), $\hat{v}$ is the (flux-normalized) downgoing field and $\hat{u}$ is the (flux-normalized) upgoing field. See Schuster and Zhou (2006) for a comprehensive overview of other options. $W(\mathbf{x}_S)$ is a weighting factor that can be used for tapering the edges of the source array (Mehta et al., 2008) or steering a virtual source in the direction of interest (Mateeva et al., 2007). We can discretize equation 1 for each frequency component as

$$\hat{\mathbf{C}} = \hat{\mathbf{U}}\mathbf{W}\hat{\mathbf{V}}^{\dagger}, \tag{2}$$

where each matrix has its columns corresponding to fixed source locations and its rows to fixed receiver locations (Berkhout, 1982). Matrix $\mathbf{W}$ is a diagonal matrix hosting the weigths $W(\mathbf{x}_S)$; $\dagger$ denotes the complex conjugate transpose.

Data-driven redatuming by inversion

Equation 1 is derived for a closed aperture of sources, while it is generally applied with one-sided illumination. Wapenaar (2006) showed that a correct Green's function can be retrieved if the medium is sufficient inhomogeneous and recording times are long. However, this assumption is often not fulfilled. Moreover, correlation-based methodology assumes the medium to be lossless. For these reasons, a different branch of interferometry emerged, where Green's functions are retrieved from a forward equation (Wapenaar et al., 2008b):

$$\hat{u}(\mathbf{x}_B \mid \mathbf{x}_S) = \int \hat{D}(\mathbf{x}_B \mid \mathbf{x}_A)\hat{v}(\mathbf{x}_A \mid \mathbf{x}_S)d\mathbf{x}_A. \tag{3}$$

Here $\hat{D}(\mathbf{x}_B \mid \mathbf{x}_A)$ is the reflection response that we aim to retrieve. We do so by discretizing equation 3 as $\hat{\mathbf{U}} = \hat{\mathbf{D}}\hat{\mathbf{V}}$, followed by least-squares inversion:

$$\hat{\mathbf{D}} \approx \hat{\mathbf{U}}\mathbf{W}\hat{\mathbf{V}}^{\dagger}\left[\hat{\mathbf{V}}\mathbf{W}\hat{\mathbf{V}}^{\dagger} + \varepsilon^2\mathbf{I}\right]^{-1}, \tag{4}$$

where ε is a stabilization factor and $\mathbf{I}$ is an identity matrix. Matrix $\mathbf{W}$ is a diagonal weighing matrix that can be used to weight the shots. The choice for $\hat{u}$ and $\hat{v}$ depend on the type of interferometry that is applied. One option is to choose $\hat{v}$ as the (flux-normalized) downgoing field and $\hat{u}$ as the (flux-normalized) upgoing field (Wapenaar et al., 2008b). Another option is to choose for $\hat{v}$ the time-gated direct field and for $\hat{u}$ the full field (van der Neut, 2009). The latter choice can be seen as the muli-dimensional deconvolution-based variant of the virtual source method.

Resolution

Equations 2 and 4 are closely related and can be combined as $\hat{\mathbf{C}} = \hat{\mathbf{D}}\hat{\mathbf{\Gamma}}$, where $\hat{\mathbf{\Gamma}} = \hat{\mathbf{V}}\mathbf{W}\hat{\mathbf{V}}^{\dagger}$. Or, in integral notation:

$$\hat{C}(\mathbf{x}_B \mid \mathbf{x}_A) = \int_{S_R} \hat{D}(\mathbf{x}_B \mid \mathbf{x}'_A)\hat{\Gamma}(\mathbf{x}'_A \mid \mathbf{x}_A)d\mathbf{x}'_A, \tag{5}$$

$$\hat{\Gamma}(\mathbf{x}'_A \mid \mathbf{x}_A) = \int_{S_S} W(\mathbf{x}_S)\hat{v}(\mathbf{x}'_A \mid \mathbf{x}_S)\hat{v}^*(\mathbf{x}_A \mid \mathbf{x}_S)d\mathbf{x}_S. \tag{6}$$

Note from equation 5 that $\hat{C}$ is a blurred version of the more accurate response $\hat{D}$, where the resolution is governed by the so-called resolution function $\hat{\Gamma}$ (Toxopeus et al., 2008). We point out the strong resemblance of equation 5 with the point-spread function for diffraction-stack migration (Schuster and Hu, 2000; Thorbecke and Wapenaar, 2007). If the medium is laterally invariant, the resolution function becomes equivalent to the amplitude radiation pattern, as described by van der Neut and Bakulin (2009) in the FK-domain. Most ideally, $\hat{\Gamma}$ converges to a spatial and temporal delta function, meaning that the virtual source is perfectly focussed. Any other resolution function indicates blurring of the retrieved data $\hat{C}$. In some cases, data can be deblurred by incorporating the inversion (equation 4) – see van der Neut et al. (2009) for a synthetic elastic example. However, it remains to be seen if this inversion can be stabilized in poorly illuminated areas. We argue that, instead of computing the inverse of $\hat{\mathbf{\Gamma}}$, the resolution function can also be used to diagnose the quality of virtual source focusing. The spurious artefacts and blurring effects that the inversion (equation 4) aims to correct for, can be observed from the resolution function, which can be obtained directly from the data through equation 6. Next we demonstrate the value of the resolution function in diagnosing virtual source radiation characteristics with a synthetic salt flank example.

Acoustic salt flank example

In Figure 2a we show the velocity model of a synthetic salt flank example. 588 sources are located at the earth's

surface with 15m spacing, ranging in lateral position from 0m to 8815m. 401 receivers are located in a vertical borehole near the flank at a lateral position of 10000m, ranging in depth from 1000m to 5000m with 10m spacing. The velocity gradient in the medium gives rise to turning waves, illuminating the salt flank under various angles. Our aim is to redatum the source array from the earth's surface to the vertical receiver array using seismic interferometry with time-gated fields (van der Neut, 2009). As an example, we pick a virtual source location at 3000 m depth, in the middle of the well. The response that we aim to retrieve (modeled by placing an active source at the virtual source location) is shown in Figure 2b. Note that the top diffraction, as well as reflections from the lower and upper part of the flank, can easily be recognized. In Figure 2c and 2d we show the time-gated direct field and the scattered field, respectively, from an actual source at the earth's surface. Generating interferometric data requires cross-correlation and integration over the source array (equation 1). It has been illustrated by various authors (e.g. Mehta et al., 2008), how a summation over sources leads to constructive interference at stationary reflection points and destructive interference outside these points. In Figure 3a we show the retrieved response, using only 1 shot. Note that the events that can be found in Figure 2b appear mispositioned in Figure 3a. Stacking the first 100, 200 and 300 shots (Figures 3b-3d) leads to destructive interference of these events as long as the stationary points are not included, as is the case for the lower flank reflection using this part of the source array. For the upper flank reflection, constructive interference does take place within this source range, leading to correct kinematical retrieval. Note that for all events, the edge effects of the finite source aperture can be recognized. An alternative interpretation is that the virtual source focuses better with increasing the source array. To illustrate this, we study the resolution function in the time-space domain. For 1 shot we find a very poor focusing at the virtual source location (Figure 4a), meaning that the retrieved data is largely mispositioned in time and space, as we saw in Figure 3a. Stacking more sources leads to better focusing at the virtual source location (Figures 4b-4d). Note that the edges of the source array still have a strong imprint on the resolution function, causing the edge effects in the retrieved data that we can clearly see in Figure 3d. To remove these edge effects, it is general practice to apply a taper to the source array (Mehta et al., 2008). In the following analysis, we show how such a taper can be effectively designed with the help of the resolution function. In Figure 5a-d we show four functions $W(\mathbf{x}_S)$ that can be applied to the total source array of 588 shots. In situation (a) no taper is applied. By studying the retrieved reflection response (Figure 6a), we can still see the edge effects of the source array clearly, even after completing the 588 shots stack. The reason for this can be easily understood by studying the resolution function – see Figure 7a. Notice the defocused 'legs' that smear out the data. Applying stronger tapering, we find the spurious events reduced (Figures 6b-d), which can be attributed to the improved focusing as can be observed in Figures 7b-d. This effect can also be seen clearly in the FK-domain. Ideally the resolution function has a flat spectrum in this domain (equivalent of a delta function in the time-space domain). Without tapering, however, we see that the edges of the spectrum are overilluminated (Figure 8a). Tapering reduces these side-effects (Figures 8b-d), leading to better focusing, but also to spatial spectrum narrowing. This latter effect can be seen in the retrieved data in Figure 6d too, where the amplitudes of the lower flank reflection are relatively weakened. The resolution function can be used to analyze these effects directly from the time-gated wavefields, without knowledge of the actual reflectors.

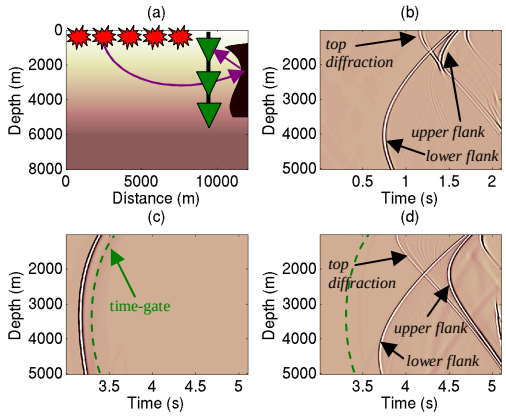

Figure 2: a) Velocity model with cartoon of a turning wave in purple, sources in red and receivers in green; velocities range from 1900 m/s (white) to 4500 m/s (black); b) reference response, with an actual source at 3000m depth in the receiver array; c) time-gated part of a typical shot record; d) scattered part of a typical shot record.

Conclusion

We derived a resolution function for redatuming source locations by correlation-based interferometry for general inhomogeneous dissipative media. This function can be estimated directly from the data if multiple downhole receivers are available. The resolution function can be used to diagnose the quality of the retrieved reflection response.

Acknowledgements

This work was supported by the Dutch Technology Foucndation STW, applied science division of NWO and the Technology Program of the Ministry of Economic Affairs (grant DCB.7913).

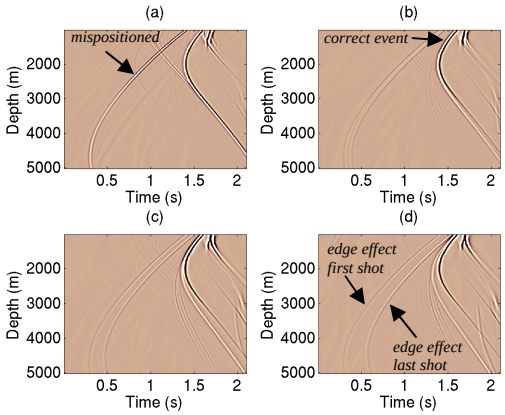

Figure 3: Retrieved shot record after stacking a) 1 shot, b) 100 shots, c) 200 shots and d) 300 shots.

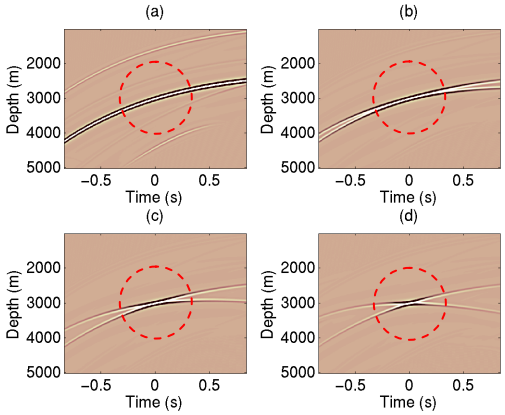

Figure 4: Resolution function after stacking a) 1 shot, b) 100 shots, c) 200 shots and d) 300 shots.

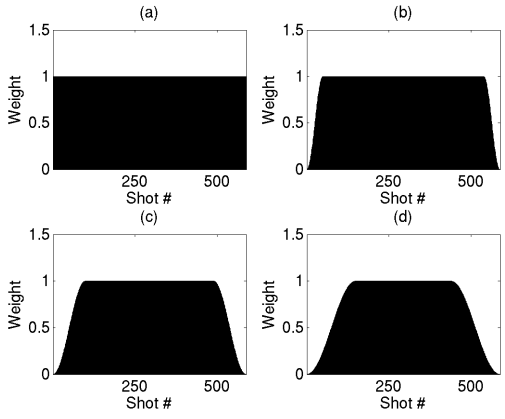

Figure 5: Four types of tapers as a function of the shot number; we refer to these tapers as (a) – (d).

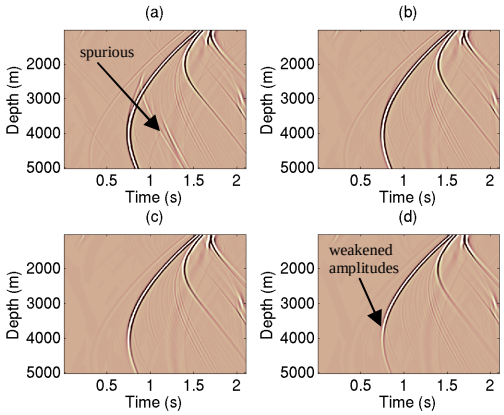

Figure 6: Retrieved shot record after stacking all 588 shots for tapers (a)-(d).

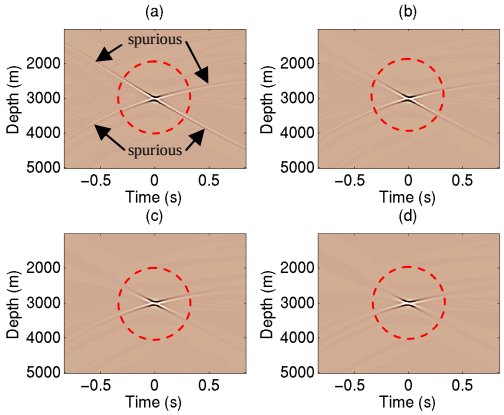

Figure 7: Resolution function after stacking all 588 shots for tapers (a)-(d).

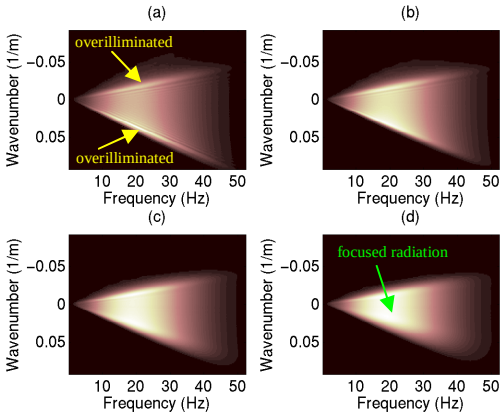

Figure 8: Resolution function in the FK domain after stacking all 588 shots for tapers (a)-(d).

EDITED REFERENCES

Note: This reference list is a copy-edited version of the reference list submitted by the author. Reference lists for the 2009 SEG Technical Program Expanded Abstracts have been copy edited so that references provided with the online metadata for each paper will achieve a high degree of linking to cited sources that appear on the Web.

REFERENCES

Bakulin, A., and R. Calvert, 2006, The virtual source method: Theory and case study: Geophysics, **71**, no. 4, SI139–SI150.

Berkhout, A. J., 1982, Seismic migration. imaging of acoustic energy by wave field extrapolation: Elsevier.

Ferrandis, J., A. Mateeva, P. Jorgensen, and J. Lopez, 2009, Application of virtual-source technology to the Zuidwending gas storage project: The Leading Edge, **28**, 296–301.

Holvik, E., and L. Amundsen, 2005, Elimination of the overburden response from multicomponent source and receiver seismic data, with source designature and decomposition in PP-, PS-, SP- and SS-wave response: Geophysics, **70**, no. 2, SI11–SI21.

Hornby, B. E., and J. Yu, 2007, Interferometric imaging of a salt flank using walkaway VSP data: The Leading Edge, **26**, 760–763.

Mateeva, A., J. Ferrandis, A. Bakulin, P. Jorgensen, C. Gentry, and J. Lopez, 2007, Steering virtual sources for salt and subsalt imaging: 77th Annual International Meeting, SEG, Expanded Abstracts, 3044–3048.

Mehta, K., A. Bakulin, J. Sheiman, R. Calvert, and R. Snieder, 2007, Improving the virtual source method by wavefield separation: Geophysics, **72**, no. 4, V79–V86.

Mehta, K, R. Snieder, R. Calvert, and J. Sheiman, 2008, Acquisition geometry requirements for generating virtual-source data: The Leading Edge, **27**, 620–629.

Minato, S., K. Onishi, T. Matsuoka, Y. Okajima, J. Tsuchiyama, D. Nobuoka, H. Azuma, and T. Iwamoto, 2007, Cross-well seismic survey without a borehole source: 77th Annual International Meeting, SEG, Expanded Abstracts, 1357–1361.

Schuster, G. T., and J. Hu, 2000, Green's function for migration: continuous recording geometry: Geophysics, **65**, 167–175.

Schuster, G. T., and M. Zhou, 2006, A theoretical overview of model-based and correlation-based redatuming methods: Geophysics, **71**, no. 4, SI103–SI110.

Schuster, G. T., 2009, Seismic interferometry: Cambridge University Press.

Thorbecke, K. and K. Wapenaar, 2007, On the relation between seismic interferometry and the migration resolution function: Geophysics, **72**, no. 6, T61–T66.

Toxopeus, G., J. Thorbecke, K. Wapenaar, S. Petersen, E. Slob, and J. Fokkema, 2008, Simulating migrated and inverted seismic data by filtering a geologic model: Geophysics, **73**, no. 2, T1–T10.

Van der Neut, J., 2009, Seismic interferometry by multi-dimensional deconvolution with time-gated wavefields: 71st Annual Meeting, EAGE, Extended Abstracts, X041.

Van der Neut, J. and A. Bakulin, 2009, Estimating and correcting the amplitude radiation pattern of a Virtual Source: Geophysics, 74, no. 2, SI27–SI36.

Van der Neut, J., and K. Wapenaar, 2009, Controlled-source elastodynamic interferometry by cross-correlation of decomposed wavefields: 71st Conference & Exhibition, EAGE, Expanded Abstracts, X044.

Van der Neut, J., K. Wapenaar, and M. K. Sen, 2009, Controlled-source seismic interferometry by multi-dimensional deconvolution applied to a laterally varying elastic model: 4th North African/Mediterranean Petroleum and Geosciences Conference & Exhibition, 4935.

Vasconcelos, I. and R. Snieder, 2008a, Interferometry by deconvolution: Part 1 – theory for acoustic waves and numerical examples: Geophysics, **73**, no. 3, S115-S128.

Vasconcelos, I., R. Snieder, and B. Hornby, 2008b, Imaging internal multiples from subsalt VSP data – examples of target-oriented interferometry: Geophysics, **73**, no. 4, S157–S168.

Wapenaar, K., J. Fokkema, and R. Snieder, 2005, Retrieving the Green's function in an open system by cross-correlation: A comparison of approaches: Journal of the Acoustical Society of America, 118, 2783–2786.

Wapenaar, K., 2006, Green's function retrieval by cross-correlation in case of one-sided illumination: Geophysical Research Letters, 33, L19304.

Wapenaar, K., D. Draganov and J. Robertsson (eds), 2008a, Seismic interferometry: History and present status: SEG, Geophysics Reprint Series 26.

Wapenaar, K, E. Slob, and R. Snieder, 2008b, Seismic and electromagnetic controlled-source interferometry in dissipative media: Geophysical Prospecting, **56**, 419–434.

Wapenaar, K., J. van der Neut, E. Ruigrok, D. Draganov, E. Slob, J. Thorbecke, and R. Snieder, 2008c, Seismic interferometry by cross-correlation or deconvolution?: 78th Annual International Meeting, SEG, Expanded Abstracts, 2731–2736.